

Supporting Information for

A Far-Red Emitting Probe for Unambiguous Detection of Mobile Zinc in Acidic Vesicles and Deep Tissue

Pablo Rivera-Fuentes,^a Alexandra T. Wrobel,^a Mustafa Khan,^b John Georgiou,^b Thomas
T. Luyben,^{b,c} John C. Roder,^{b,c} Kenichi Okamoto,^{b,c} and Stephen J. Lippard^{a*}

^aDepartment of Chemistry, Massachusetts Institute of Technology, Cambridge, MA 02139;

^bLunenfeld-Tanenbaum Research Institute, Mount Sinai Hospital, Toronto, ON, Canada M5G

1X5; ^cDepartment of Molecular Genetics, Faculty of Medicine, University of Toronto, Toronto,
ON, Canada M5S 1A8.

lippard@mit.edu*

Contents

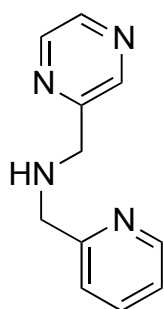
General Materials and Methods	S2
Synthesis	S2
Spectroscopic Methods	S3
pH Titration, Metal Selectivity, and Dissociation Constant	S4
Kinetic Experiments.....	S5
Cell Culture and Staining Procedures	S5
Fluorescence Microscopy	S6
Colocalization Analysis	S7
Hippocampal Slice Preparation and Staining	S7
Two-photon Microscopy.....	S8
Figure S1. ¹ H NMR spectrum of SpiroZin2.	S10
Figure S2. ¹³ C NMR spectrum of SpiroZin2.	S10
Figure S3. Absorption and fluorescence of SpiroZin2	S11
Figure S4. Determination of the dissociation constant (K_d) of SpiroZin2	S11
Figure S5. pH Profile of SpiroZin2.....	S12
Figure S6. Metal selectivity of SpiroZin2.....	S12
Figure S7. Turn-on kinetics of SpiroZin2.....	S13
Figure S8. Turn-off kinetics of SpiroZin2	S13
Figure S9. Live cell imaging of MIN6 cells using SpiroZin2.	S14
Figure S10. In vivo two-photon excitation profile of SpiroZin2.	S14
Figure S11. Colocalization of ZP1 and SpiroZin2 in mossy fiber boutons	S15
References.....	S15

General Materials and Methods

All reagents were purchased from commercial sources and used as received. Compounds **1** and **2** were prepared according to published methods.^{1,2} Solvents were purified and degassed by standard procedures. NMR spectra were acquired on a Varian Inova-500 or a Varian Inova-300 instrument. ¹H NMR chemical shifts are reported in ppm relative to SiMe₄ ($\delta = 0$) and were referenced internally with respect to residual protons in the solvent ($\delta = 3.31$ for CH₃OH). Coupling constants are reported in Hz. ¹³C NMR chemical shifts are reported in ppm relative to SiMe₄ ($\delta = 0$) and were referenced internally with respect to solvent signal ($\delta = 49.00$ for CD₃OD). Low-resolution mass spectra (LRMS) were acquired on an Agilent 1100 Series LC/MSD Trap spectrometer (LCMS), by using electrospray ionization (ESI). High-resolution mass spectrometry (HR-ESI-MS) was conducted by staff at the MIT Department of Chemistry Instrumentation Facility on a Bruker Daltonics APEXIV 4.7 T FT-ICR-MS instrument. Semipreparative HPLC separations were carried out on an Agilent 1200 HPLC instrument with a multiwavelength detector and automated fraction collector using a C18 reverse stationary phase (Zorbax-SB C18, 5 μ m, 9.5 \times 250 mm) and a mobile phase composed of two solvents (A: 0.1% (v/v) trifluoroacetic acid (TFA) in H₂O; B: 0.1% (v/v) TFA in CH₃CN). The IUPAC name of SpiroZin2 is provided and was determined using CS ChemBioDrawUltra 12.0.

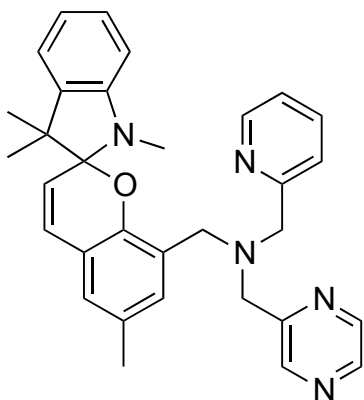
Synthesis

1-(Pyrazin-2-yl)-N-(pyridin-2-ylmethyl)methanamine (**3**)



Pyrazine-2-carbaldehyde (1 g, 9.25 mmol) was dissolved in CH₃OH (90 mL). Pyridin-2-ylmethanamine (953 μ L, 9.25 mmol) was added by syringe and the solution was stirred at 25 $^{\circ}$ C for 30 min. Solid NaBH₄ (1.06 g, 27.76 mmol) was rapidly added to the solution and the mixture was stirred at 25 $^{\circ}$ C for 2 h. The solvent was evaporated under reduced pressure and the residue was suspended in H₂O (20 mL). Solid Na₂CO₃ was added until the suspension reached pH \sim 10. The mixture was extracted with CH₂Cl₂ (3 \times 30 mL) to give the product as a pale-yellow oil (1.81 g, 98%). The spectroscopic properties of the product match those reported for this compound.³ ¹H NMR (300 MHz, CDCl₃): 3.98 (d, ³J = 12 Hz, 4H), 7.14 (t, ³J = 6 Hz, 1H), 7.30 (d, ³J = 6 Hz, 1H), 7.62 (m, 1H), 8.42 (s, 1H), 8.49 (s, 1H), 8.53 (d, ³J = 6 Hz, 1H), 8.62 (s, 1H). LRMS (ESI). Calcd for [C₁₁H₁₃N₄]⁺: 201.2, found 201.1.

1-(Pyrazin-2-yl)-*N*-(pyridin-2-ylmethyl)-*N*-((1',3',3',6-tetramethylspiro[chromene-2,2'-indolin]-8-yl)methyl)methanamine (SpiroZin2)



Compound **2** (100 mg, 0.54 mmol) was added to a Schlenk flask that was evacuated and refilled with nitrogen three times. A solution of amine **3** (99 μ L, 0.54 mmol) and DIPEA (282 μ L, 1.62 mmol) in EtOH (5 mL) was added to the flask. The mixture was stirred at 25 $^{\circ}$ C for 1 h. Compound **1** (171 mg, 0.57 mmol) was added as a solid and the mixture was heated to reflux for 2 h. The solution was decanted and evaporated under reduced pressure. The

residue was filtered through a plug of SiO₂ eluting with CH₂Cl₂ to give the crude compound as a yellow solid (125 mg, 46%). Further purification was carried out by RP-HPLC according to the following protocol: constant flow rate 3 mL min⁻¹; isocratic flow 2% B, 0–5 min; gradient 2–35 % B, 5–10 min; gradient 35–75% B, 10–20 min; gradient 75–95% B, 20–28 min. The product was collected between 12.5–14.5 min. All equivalent fractions recovered from independent runs were combined and lyophilized to dryness to yield SpiroZin2 as a trifluoroacetate salt. ¹H NMR (300 MHz, CD₃OD): 1.14 (s, 3H), 1.26 (s, 3H), 2.19 (s, 3H), 2.68 (s, 3H), 3.40 (d, ²*J* = 12 Hz, 1H), 3.57 (d, ²*J* = 12 Hz, 1H), 3.65 (s, 4H), 5.74 (d, ³*J* = 12 Hz), 6.46 (d, ³*J* = 9 Hz, 1H), 6.75 (dd, ⁴*J* = 3 Hz, ³*J* = 6 Hz, 1H), 6.80 (dd, ⁴*J* = 3 Hz, ³*J* = 6 Hz, 1H), 6.88 (d, ³*J* = 9 Hz), 6.94 (d, ³*J* = 3 Hz, 1 H), 7.02–7.08 (m, 2H), 7.20 (m, 1H), 7.38 (d, ³*J* = 9 Hz, 2H), 7.65 (m, 1H), 8.33 (m, 2H), 8.40 (m, 1H), 8.48 (d, ³*J* = 3 Hz, 1H). ¹³C NMR (125 MHz, CD₃OD): 19.67, 26.18, 26.21, 33.79, 33.84, 52.93, 56.96, 57.48, 58.07, 64.50, 115.09, 122.58, 123.20, 124.42, 124.79, 125.73, 129.81, 129.84, 130.04, 130.41, 138.32, 141.84, 142.56, 143.99, 144.10, 144.34, 145.59, 145.84, 145.87, 150.17, 153.47, 155.67, 157.35, 183.34. HRMS (ESI). Calcd for [C₃₂H₃₄N₅O]⁺: 504.2758, found 504.2774.

Spectroscopic Methods

Aqueous solutions were prepared by using de-ionized water with resistivity 18.2 m Ω cm⁻¹, obtained using a Milli-Q water purification system. Solvents were purchased from Aldrich and used as received. Piperazine-*N,N'*-bis(2-ethanesulfonic acid) (PIPES) and 99.999% KCl were purchased from Calbiochem. Stock solutions of SpiroZin2 in DMSO were prepared at a concentration of 4 mM and stored at –20 $^{\circ}$ C in 1 mL aliquots and

thawed immediately before each experiment. All spectroscopic measurements were conducted in aqueous buffer containing 50 mM PIPES (pH 7) and 100 mM KCl. UV-visible spectra were acquired employing a Cary 50 spectrometer using quartz cuvettes from Starna (1 cm path length). Fluorescence spectra were acquired using a Photon Technology International fluorimeter. All measurements were conducted at 37 °C, unless it is stated otherwise, maintained by circulating water baths. Extinction coefficients were determined in the 1-to-5 μM range in aqueous buffer. Fluorescence quantum yields were measured by using 1-to-5 μM sensor aqueous buffer solutions, exciting at 518 nm. Fluorescence emission spectra were integrated from 530 to 800 nm. The quantum yield calculation was standardized to resorufin, which has a quantum yield of 0.74 at pH 9.5, $\lambda_{\text{ex}} = 570 \text{ nm}$.⁴

pH Titration, Metal Selectivity, and Dissociation Constant

To determine the effect of pH on the fluorescence emission of SpiroZin2, 5 μM solutions of the probe were prepared in aqueous buffer (citric acid/ Na_2HPO_4 ; pH 3–6 and 50 mM PIPES, 100 mM KCl; pH 7) and the pH was verified using a Mettler Toledo FE20 pH meter. Fluorescence spectra were recorded before and after addition of 100 equiv of ZnSO_4 , and the intensities were normalized with respect to 5 μM SpiroZin2 at pH 7 before addition of ZnSO_4 .

The metal selectivity of SpiroZin2 was measured in PIPES-buffered solutions (pH 7) containing 5 μM SpiroZin2. To each solution, 100 equiv of NaCl, MgCl_2 , CaCl_2 , CdSO_4 , NiCl_2 , CuCl_2 , MnCl_2 , or CoCl_2 were added and the fluorescence intensity measured. To the same solutions, 100 equiv of ZnSO_4 were added and the fluorescence intensity recorded. In each case, the fluorescence intensity was normalized with respect to 5 μM SpiroZin2 in aqueous buffer.

To determine the apparent dissociation constant (K_d), PIPES-buffered solutions containing 1 mM ethylene glycol tetraacetic acid (EGTA) and 5 μM SpiroZin2 were prepared. The concentration of buffered free Zn^{2+} was varied from 0 to 50 nM by addition of ZnSO_4 . The total amount of ZnSO_4 necessary to achieve the desired concentration of buffered free Zn^{2+} was determined using the web-based program Maxchelator (<http://maxchelator.stanford.edu/webmaxc/webmaxcS.htm>). The solutions containing SpiroZin2 and the desired amount of free Zn^{2+} were equilibrated in the dark for 24 h, although shorter equilibration times might suffice. The fluorescence of these solutions was measured and normalized with respect to 5 μM SpiroZin2 in the presence of 100

equiv of ZnSO₄. The normalized fluorescence responses (R) were plotted against the concentration of free Zn²⁺ (Figure S4) and the resulting data were fit to the equation $R = B[Zn]/(K_d + [Zn])$, where $B = 1$. Minimization of this equation gave the values $K_d = 3.6(4)$ nM and $R^2 = 0.991$.

Kinetic Experiments

The ring-opening reaction of SpiroZin2 in the presence of Zn²⁺ was monitored by stopped-flow fluorescence spectroscopy using a Hi-Tech Scientific SF-61 DX2 stopped-flow spectrophotometer with a Xe lamp. Upon excitation at $\lambda_{ex} = 518$ nm, the fluorescence was measured by using a 590 long-pass emission filter. Solutions containing 5 μ M SpiroZin2 and 500 μ M ZnSO₄ were prepared in aqueous buffer (50 mM PIPES, 100 mM KCl, pH 7). The reactions were maintained at 25 °C because the fast step of the reaction could not be observed at 37 °C. Data points were collected on a logarithmic time scale (0.001-10 s). A dead time determination indicated that the first usable data points occurred between 1 and 2 ms and the raw data were truncated accordingly. The data used for analysis are averages of eight independent measurements and were fit to a double exponential function: $F = F_0 + B_1 \exp[k_1 t] + B_2 \exp[k_2 t]$, where F is the measured fluorescence intensity, F_0 the initial fluorescence, k_1 and k_2 the rate constants of the two steps, t is time, and B_1 and B_2 are constants. Minimization of this equation gave the values $k_1 = 69.4(9)$ s⁻¹, $k_2 = 0.34(6)$ s⁻¹, $R^2 = 0.9924$.

The ring-closing process was monitored by fluorescence spectroscopy. A solution containing 5 μ M SpiroZin2 and 5 μ M ZnSO₄ was prepared and allowed to react in the dark for 5 min. The fluorescence of this solution was measured and 100 equiv of EDTA were added. The fluorescence intensity at $\lambda_{em} = 645$ nm ($\lambda_{ex} = 518$ nm) was measured every 1 s at 37 °C. Fluorescence intensities at each time point were plotted against time and the data were fit to a single exponential function: $F = F_0 + B_1 \exp[k_1 t]$, where F is the fluorescence intensity, F_0 the initial fluorescence, k_1 the rate constant, t is time, and B_1 a constant. Minimization of this equation gave the values $k_1 = 0.0144(2)$ s⁻¹ and $R^2 = 0.9985$.

Cell Culture and Staining Procedures

HeLa cells were cultured in Dulbecco's modified Eagle medium (DMEM; Cellgro, MediaTec, Inc.) supplemented with 10% fetal bovine serum (FBS; HyClone), 1% penicillin-streptomycin, 1% sodium pyruvate, and 1% L-glutamine. MIN6 cells were cultured in DMEM containing 25 mM D-glucose, 15 % FBS, 1% penicillin-streptomycin,

and 70 μM β -mercaptoethanol. The cells were grown to 90% confluence at 37 °C with 5% CO_2 before being passed and plated onto poly-D-lysine coated plates 24 h before imaging. Cells used were between passage numbers 2-15. A confluence level of 50% or higher was reached at imaging. The growth medium was replaced with dye-free DMEM containing 5 μM SpiroZin2, 2 μM Hoechst 33258 nuclear stain, and 2 μM LysoTracker Green® (Life Technologies), and the cells were incubated for 30 min. Cells were rinsed with PBS buffer (2 x 2 mL) prior to addition of fresh dye-free DMEM (2 mL) and mounted on the microscope.

Fluorescence Microscopy

Imaging experiments that employed cultured cells were performed using a Zeiss Axiovert 200M inverted epifluorescence microscope equipped with an EM-CCD digital camera (Hamamatsu) and a MS200 XY Piezo Z stage (Applied Scientific Instruments). The light source was a X-Cite 120 metal-halide lamp (EXFO) and the fluorescence images were obtained using an oil-immersion objective at 100 \times magnification. The fluorescence filter sets used are defined as blue: excitation G 365 nm, beamsplitter FT 395 nm, emission band pass (BP) 445/50 nm; green: excitation BP 470/40 nm, beamsplitter FT 495 nm, emission 525/50 nm; and red: BP 550/25 nm, beamsplitter FT 570 nm, emission BP 605/70 nm. The microscope was operated using Volocity software (Perkin-Elmer).

The exposure times for acquisition of fluorescence images were kept constant for each series of images at each channel. To measure Zn^{2+} -induced fluorescence changes in HeLa cells, the medium in the plate was replaced with dye-free DMEM containing 30 μM ZnCl_2 and 60 μM pyrithione and images were recorded after 10 min. To reverse the effect of zinc, the cells were exposed to dye-free DMEM containing 50 μM TPEN for 10 min. Chelation of intracellular mobile zinc in MIN6 cells was performed by treating the cells with dye-free DMEM containing 50 μM TPEN for 10 min. Insulin and zinc release from MIN6 cells was induced by bathing the cells in dye-free DMEM supplemented with 50 mM KCl and 20 mM glucose. All these experiments were carried out on the stage of the microscope. Quantification of fluorescence intensity was performed using ImageJ (version 1.45, NIH). The whole cell was selected as the region of interest. The integrated fluorescence from the background region was subtracted from the cell body region.

Colocalization Analysis

Point-spread functions (PSF) for wide-field green and red channels were calculated using Volocity software with the following parameters: lateral spacing in X-Y = 0.067 μm , refractive index of the medium $\eta = 1.51$, numerical aperture = 1.4, and emission wavelengths $\lambda_{\text{green}} = 518 \text{ nm}$ and $\lambda_{\text{red}} = 650 \text{ nm}$. These calculated PSFs were used to restore the images iteratively to a 95% confidence level. Deconvoluted images of green (LysoTracker Green) and red (SpiroZin2) channels were overlaid, and the signal threshold was defined by selecting an empty region of the plate as background. The correlation and colocalization coefficients Pearson's (r_p) and Manders' (M_{green} and M_{red})⁵ were calculated using the whole cell body as the region of interest.

Pearson's correlation coefficient:

$$r_p = \frac{\sum_i (G_i - G_{\text{avg}}) \cdot (R_i - R_{\text{avg}})}{\sqrt{\sum_i (G_i - G_{\text{avg}})^2 \cdot \sum_i (R_i - R_{\text{avg}})^2}}$$

In this equation, G_i is the intensity of green fluorescent in a given pixel, G_{avg} the average intensity in the green channel, R_i the intensity of red fluorescence in a given pixel, and R_{avg} the average intensity in the red channel.

Manders' colocalization coefficient:

$$M_{\text{green}} = \frac{\sum_i G_{i,\text{coloc}}}{\sum_i G_i}$$

In this equation, $G_{i,\text{coloc}} = G_i$ if $R_i > 0$ and $G_{i,\text{coloc}} = 0$ if $R_i = 0$. G_i and R_i are the same variables defined before for the Pearson's coefficient. M_{red} can be defined in an analogous manner.

Hippocampal Slice Preparation and Staining

Hippocampal slices were prepared from 60-80 day old mice as described previously.⁶ GFP mice (Thy1-GFP, line M)⁷ were obtained from Jackson labs and housed in the animal facility. $ZnT3^{+/-}$ mice (obtained from Dr. Gleb Shumyatsky, Rutgers University) were bred to obtain $ZnT3^{-/-}$ and $ZnT3^{+/+}$ mice as described previously.⁸ For Zn^{2+} staining, the hippocampal slices were bathed in artificial cerebrospinal fluid (ACSF) containing 100 μM SpiroZin2 or 25 μM ZP1, 119 mM NaCl, 3 mM KCl, 1.25 mM NaH_2PO_4 , 26

mM NaHCO₃, 11 mM D-glucose, 2.5 mM CaCl₂, 1.3 mM MgCl₂ for 15 minutes and gassed with 95% O₂/5% CO₂ at room temperature in a 1.5 mL centrifuge tube. The slices were then placed in the microscope chamber and washed for 10 minutes in ACSF.

Two-photon Microscopy

All two-photon fluorescence imaging was carried out using a custom-made two-photon laser scanning microscope based on an Olympus FV1000MPE/BX51WI microscope, equipped with a 60× objective lens (NA1.0, LUMPLFLN, Olympus) and MaiTai HP DeepSee laser (Spectra-Physics). Stained hippocampal slices were imaged using 860 nm (10 mW) two-photon excitation (TPE) to obtain images with minimal background (Figure S10). GFP and ZP1 were imaged using a 495-540 nm emission filter. SpiroZin2 was imaged using a 603.5-678.5 nm emission filter. Image stacks were composed using 40-60 sections taken at 1 μm intervals. For SpiroZin2 TPE profile, the SpiroZin2 stained hippocampal slices were imaged at 750-1000 nm (two-photon excitation, 10 mW) and the fluorescence intensity of the mossy fiber boutons were measured using the intensity mean of the spots function (Imaris, Bitplane). Signal from hippocampal regions adjacent to the mossy fibers was also measured as background signal of SpiroZin2 in hippocampal slices. To measure fluorescence profiles of zinc sensors along the z-axis of hippocampal tissues, the stained hippocampal slices were imaged and stacked using 40-60 sections at 4 μm intervals. Representative images were prepared after background subtraction and Gaussian filtering in Photoshop CS6 (Adobe). Three-dimensional representative images were projected in two-dimensions using Imaris (Bitplane). For x-z images, the stacks were merged in two dimensions also using Imaris. TPE cross sections were carried out at room temperature and in aqueous solutions containing 100 μM ZnCl₂ using the following formula:

$$\sigma_{2\text{new}}(\lambda)\eta_{2\text{new}} = \frac{\Phi_{\text{sat}}\sigma_{2\text{sat}}(\lambda)\eta_{2\text{sat}}C_{\text{sat}}\langle P_{\text{sat}}(t) \rangle^2 \langle F(t) \rangle_{\text{new}} n_{\text{sat}}}{\Phi_{\text{new}}C_{\text{new}}\langle P_{\text{new}}(t) \rangle^2 \langle F(t) \rangle_{\text{sat}} n_{\text{new}}}$$

where $\sigma_2(\lambda)\eta_2$ is the TPE cross section at wavelength λ , Φ is the fluorescence collection efficiency, C is the concentration, $\langle P(t) \rangle$ is the average incident power, $\langle F(t) \rangle$ is the time-averaged fluorescence emission, and n is the refractive index of the sample⁹. Time-averaged fluorescence emission was measured with a time-correlated single photon counting (TCSPC) system (PicoHarp 300, FLIM upgrade kit for Olympus FV1000MPE, SymPhoTime software; Picoquant). The TPE cross section was standardized to sulforhodamine 101, which has a cross section of 118 GM (1 GM = 10⁻⁵⁰ (cm⁴ s)/photon)

at 910 nm¹⁰. Two photon absorbance (TPA) cross sections were calculated using the following formula:

$$\sigma_{TPA}(\lambda) = \frac{\sigma_{TPE}(\lambda)}{\eta_2}$$

We assumed that the two photon quantum yield η_2 is equal to the one photon quantum yield, as has been done previously¹¹.

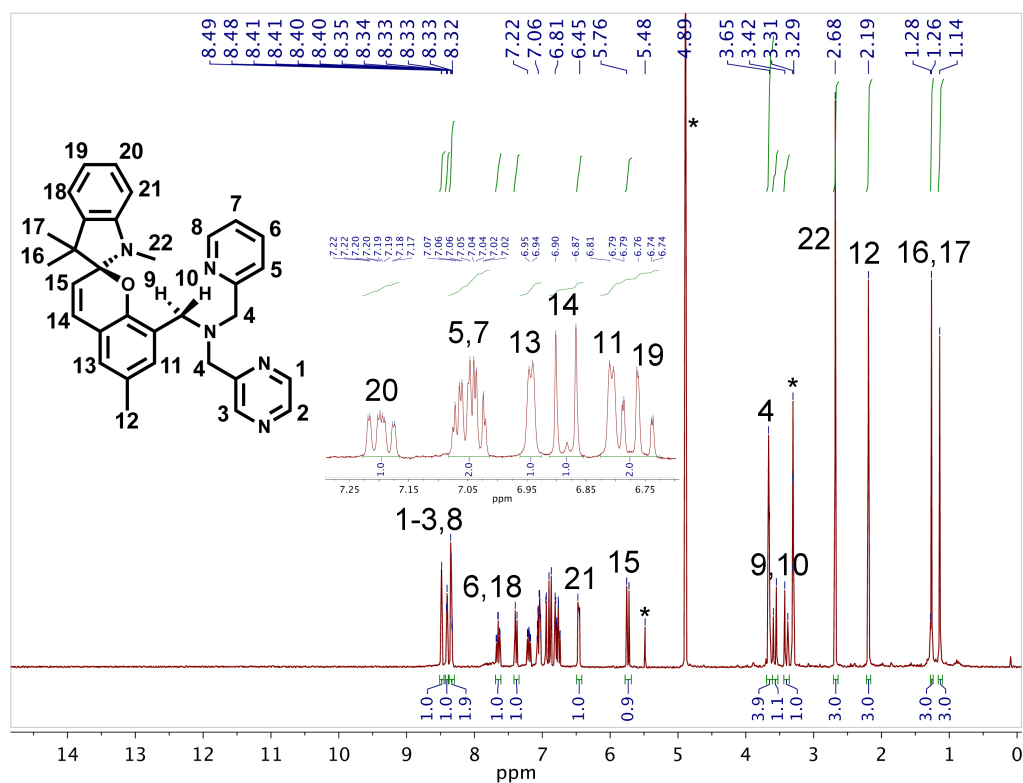


Figure S1. ^1H NMR (300 MHz, CD_3OD) spectrum of SpiroZin2. Peaks were assigned based on chemical shift and multiplicity. *Residual CH_3OH , H_2O , and CH_2Cl_2 .

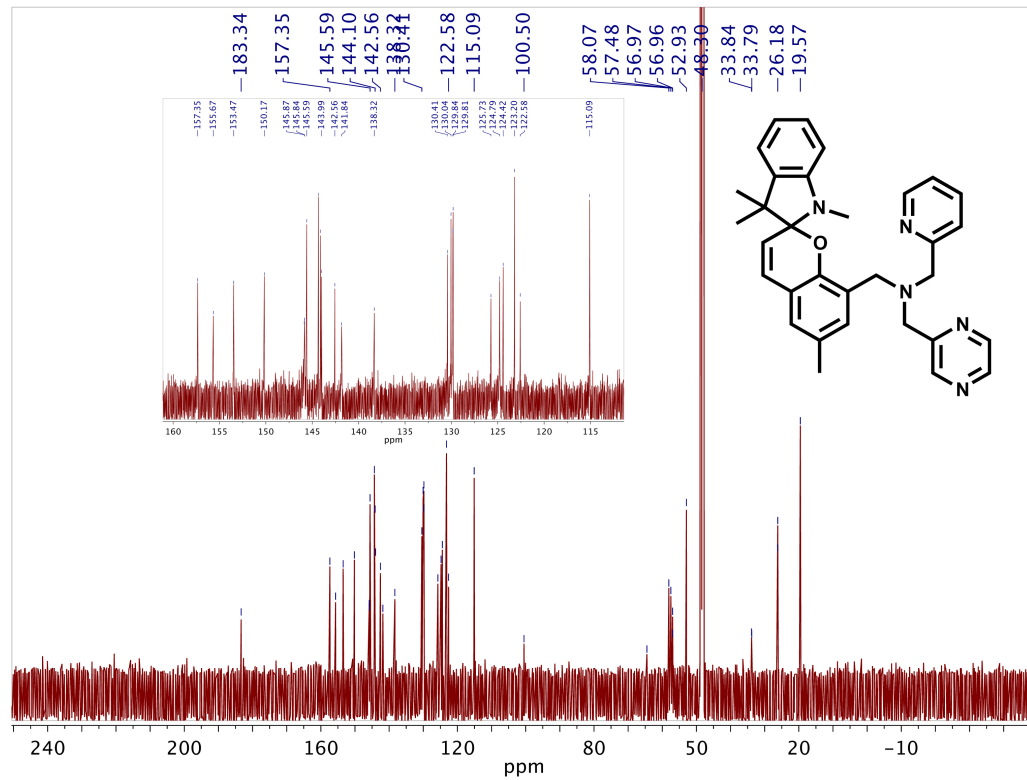


Figure S2. ^{13}C NMR (125 MHz, CD_3OD) spectrum of SpiroZin2.

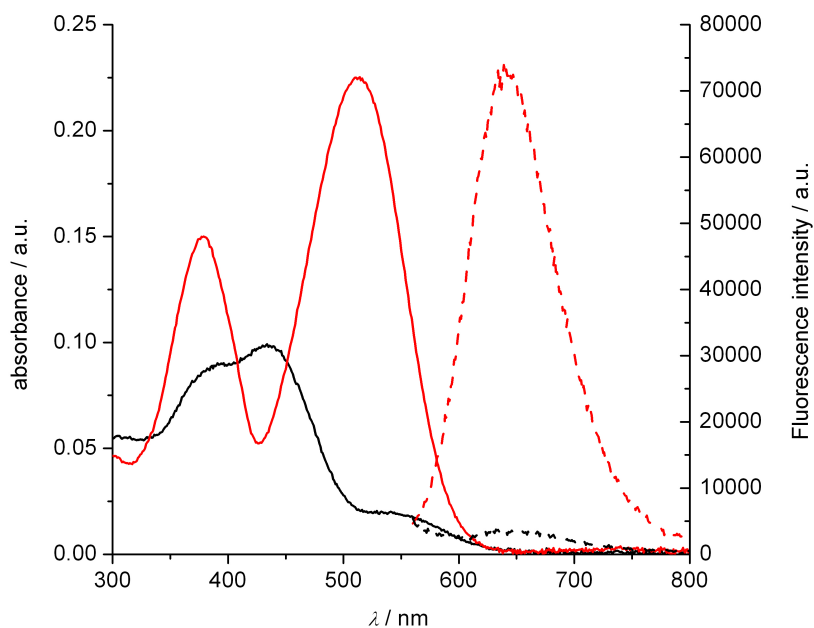


Figure S3. Absorption (solid lines) and fluorescence (dotted lines) spectra of 5 μM SpiroZin2 in aqueous buffer (50 mM PIPES, 100 mM KCl, pH 7) before (black lines) and after (red lines) addition of 100 equiv of ZnSO_4 . Photophysical properties: $\lambda_{\text{abs}} = 518 \text{ nm}$ ($3.071(1) \times 10^4 \text{ cm}^{-1} \text{ M}^{-1}$); $\lambda_{\text{em}} = 645 \text{ nm}$ (quantum yield $\phi = 0.0010(1)$).

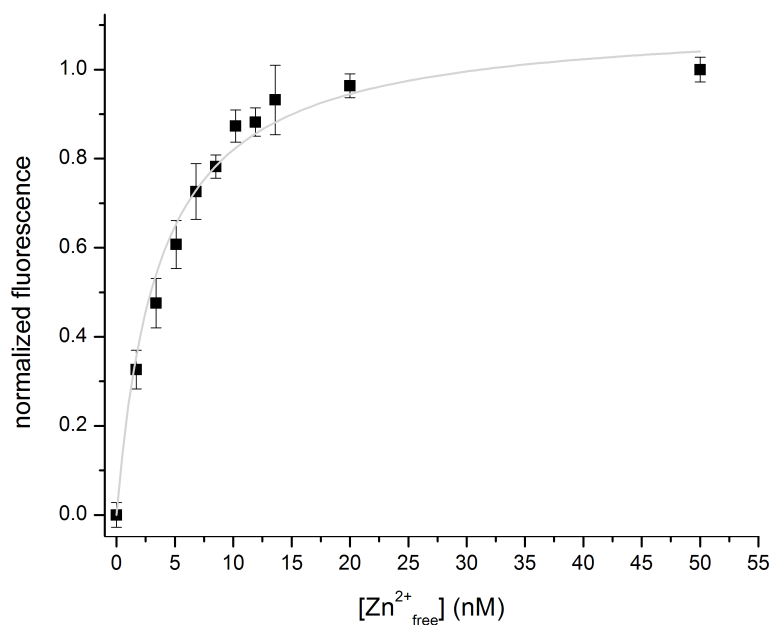


Figure S4. Determination of the dissociation constant (K_d) of SpiroZin2. Buffered solutions of Zn^{2+} were prepared using 1 mM ethylene glycol tetraacetic acid (EGTA) and ZnSO_4 . $K_d = 3.6(4) \text{ nM}$; $R^2 = 0.991$.

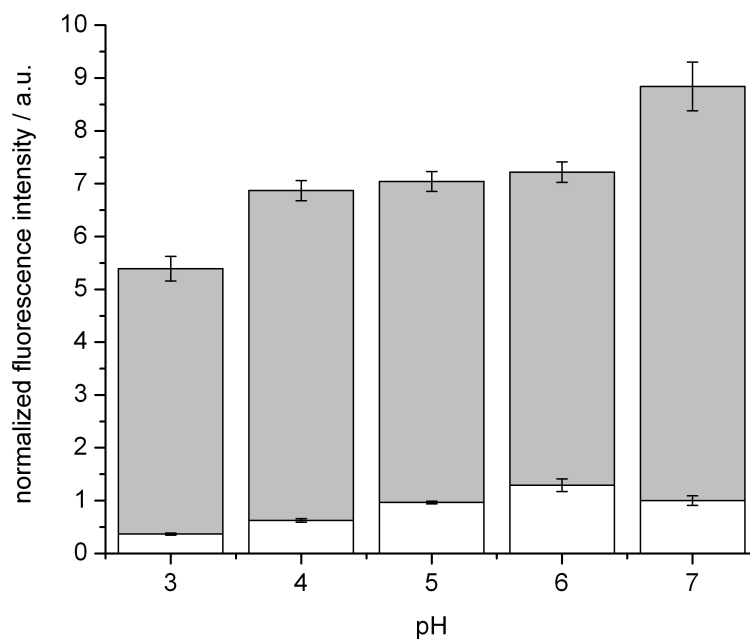


Figure S5. Fluorescence of 5 μM SpiroZin2 before (white bars) and after (grey bars) addition of 100 equiv of ZnSO_4 at varying pH values.

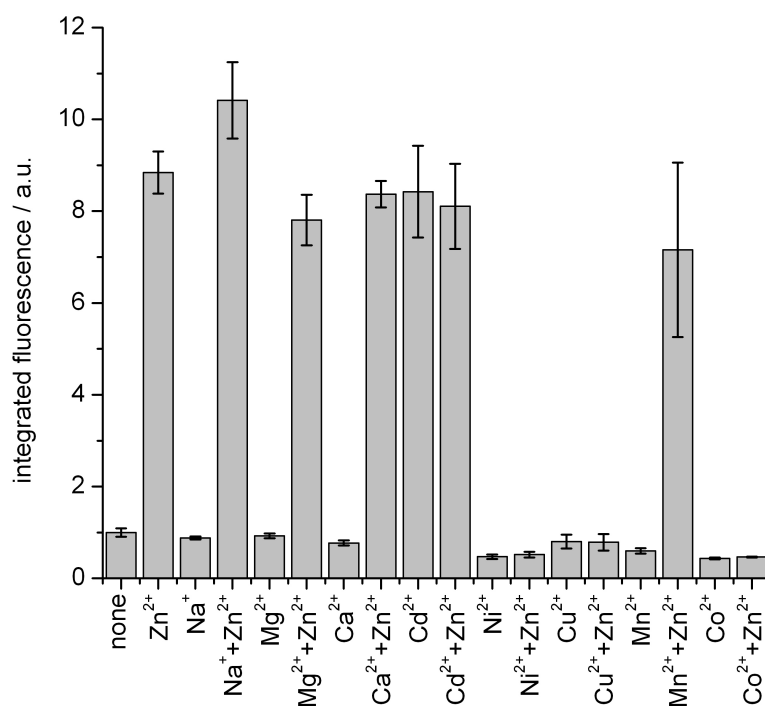


Figure S6. Metal selectivity of SpiroZin2. Integrated fluorescence intensity of 5 μM SpiroZin2 in buffer (50 mM PIPES, 100 mM KCl, pH 7). 100 equiv of the indicated analyte were added prior to addition of 100 equiv of ZnSO_4 .

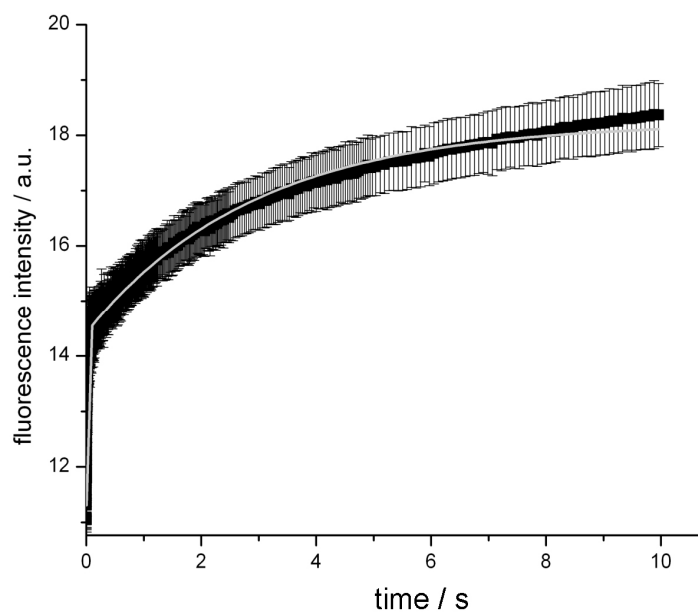


Figure S7. Turn-on kinetics of SpiroZin2 (25 °C) determined by stopped-flow fluorescence spectroscopy. Increase in fluorescence of 5 μM SpiroZin2 in aqueous buffer (50 mM PIPES, 100 mM KCl, pH 7) after addition of 100 equiv of ZnSO_4 . Kinetic parameters: $t_{1/2\text{fast}} = 14.4(2)$ ms; $t_{1/2\text{slow}} = 2.92(5)$ s. $R^2 = 0.9924$.

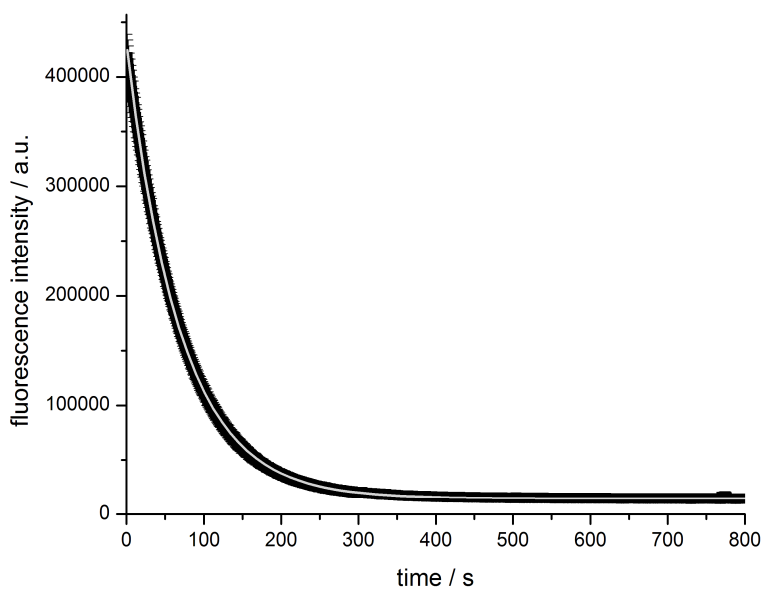


Figure S8. Turn-off kinetics of SpiroZin2 (37 °C) determined by fluorescence spectroscopy. Decrease in fluorescence (645 nm, $\lambda_{\text{ex}} = 518$ nm) of 5 μM zinc-bound SpiroZin2 in aqueous buffer (50 mM PIPES, 100 mM KCl, pH 7) after addition of 100 equiv of EDTA. Kinetic parameters: $t_{1/2} = 69.4(9)$ s; $R^2 = 0.9985$.

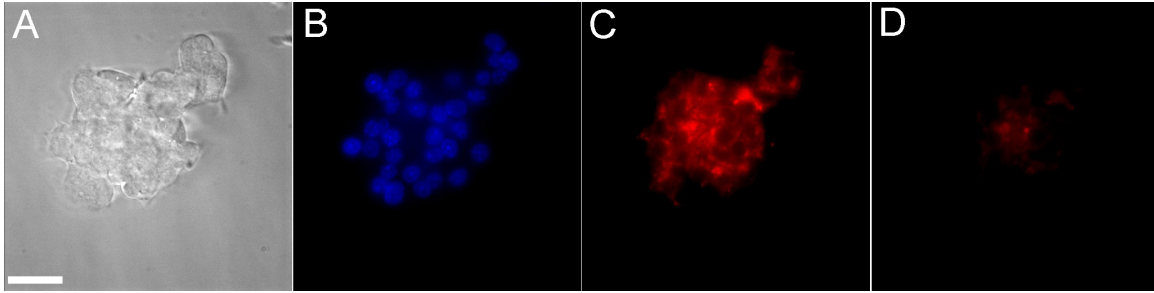


Figure S9. Live cell imaging of MIN6 cells using SpiroZin2. A) Differential interference contrast (DIC) image; B) Blue channel showing nuclei stained with Hoechst 33258; C) Red channel before any treatment; D) Red channel 20 min after stimulation of the cells with 50 μ M KCl and 20 mM glucose. Scale bar = 10 μ m

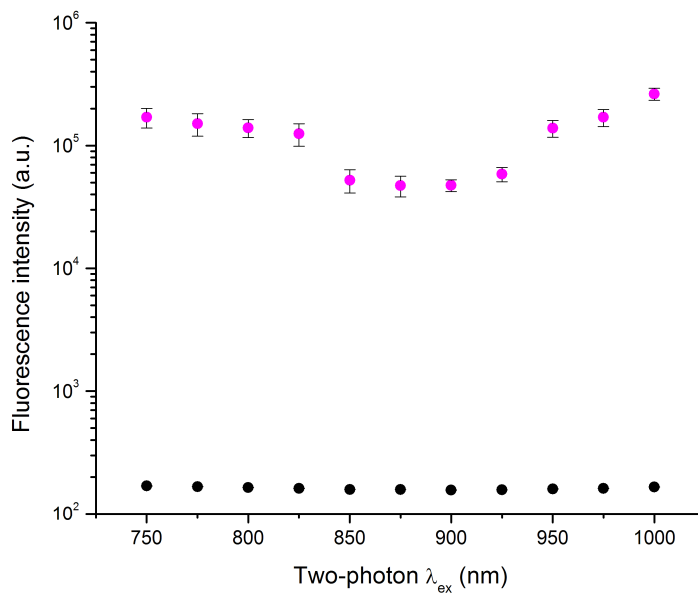


Figure S10. In vivo two-photon excitation profile of SpiroZin2. Fluorescence intensity was measured in the mossy fiber boutons (magenta) and the background regions (black) in acutely isolated mouse hippocampal slices using various two-photon excitation wavelengths. Slices were stained with 100 μ M SpiroZin2 for 10 min, and the fluorescence intensity was plotted for the average ($n = 3$). Two-photon photophysical properties: σ_{TPE} at 910 nm = 0.0740 GM; σ_{TPA} at 910 nm = 74.033 GM⁹.

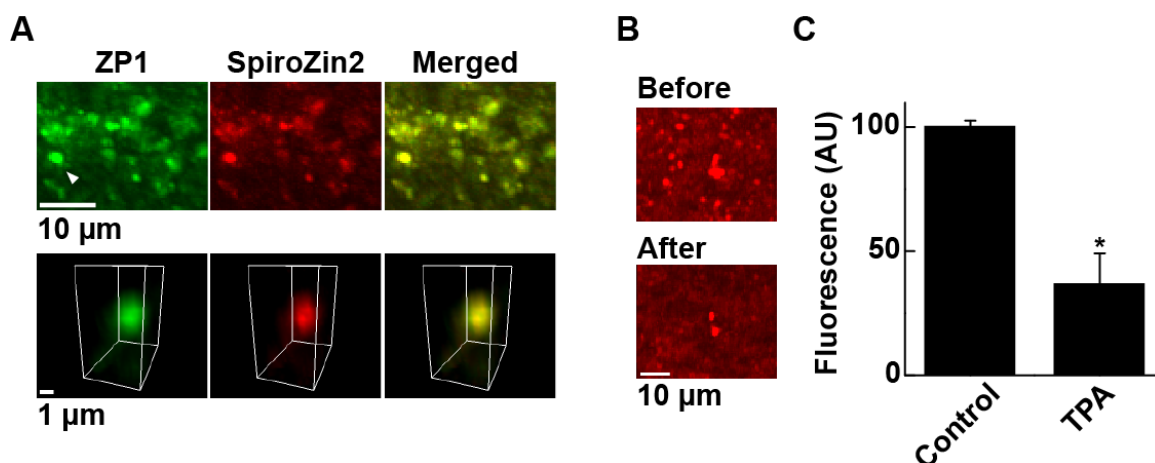


Figure S11. A) Colocalization of ZP1 (green) and SpiroZin2 (red) in mossy fiber boutons of a hippocampal slice (top panels). Enlarged, 3D view of the mossy fiber bouton indicated by a white arrow (bottom panels). B) Representative images of mossy fiber regions of slices treated with SpiroZin2. Images were obtained before and 10 min after treatment with the intracellular zinc chelator TPA (200 μM). C) Quantification of SpiroZin2 fluorescence intensity in mossy fiber regions treated with TPA. Control, $n = 3$; TPA, $n = 3$. * $P < 0.05$, paired t test. TPA = Tris(2-pyridylmethyl)amine.

References

- (1) Ueno, Y.; Jose, J.; Loudet, A.; Pérez-Bolívar, C.; Anzenbacher, P., Jr.; Burgess, K. J. *Am. Chem. Soc.* **2011**, *133*, 51-55.
- (2) Chirakul, P.; Hampton, P. D.; Bencze, Z. *J. Org. Chem.* **2000**, *65*, 8297-8300.
- (3) Zhang, X.-a.; Hayes, D.; Smith, S. J.; Friedle, S.; Lippard, S. J. *J. Am. Chem. Soc.* **2008**, *130*, 15788-15789.
- (4) Bueno, C.; Villegas, M. L.; Bertolotti, S. G.; Previtali, C. M.; Neumann, M. G.; Encinas, M. V. *Photochem. Photobiol.* **2002**, *76*, 385-390.
- (5) Manders, E. M. M.; Verbeek, F. J.; Aten, J. A. *J. Microsc.* **1993**, *169*, 375-382.
- (6) Chang, C. J.; Nolan, E. M.; Jaworski, J.; Okamoto, K. I.; Hayashi, Y.; Sheng, M.; Lippard, S. J. *Inorg. Chem.* **2004**, *43*, 6774-6779.
- (7) Feng, G. P.; Mellor, R. H.; Bernstein, M.; Keller-Peck, C.; Nguyen, Q. T.; Wallace, M.; Nerbonne, J. M.; Lichtman, J. W.; Sanes, J. R. *Neuron* **2000**, *28*, 41-51.
- (8) Cole, T. B.; Wenzel, H. J.; Kafer, K. E.; Schwartzkroin, P. A.; Palmiter, R. D. *Proc. Natl. Acad. Sci. U. S. A.* **1999**, *96*, 1716-1721.
- (9) Albota, M. A.; Xu, C.; Webb, W. W. *Appl Opt* **1998**, *37*, 7352-7356.

- (10) Mutze, J.; Iyer, V.; Macklin, J. J.; Colonell, J.; Karsh, B.; Petrusek, Z.; Schwille, P.; Looger, L. L.; Lavis, L. D.; Harris, T. D. *Biophys. J.* **2012**, *102*, 934-944
- (11) Xu, C.; Webb, W. W. *J. Opt. Soc. Am. B.*, **1996**, *13*, 481–491.